Medical Research Archives

ESMED
European Society of Medicine

OPEN ACCESS

Published: June 30, 2022

Citation: Cousins Joseph and Ayman Nada, 2022. High-Resolution Intratumoral Susceptibility Signal (ITSS) as an Adjunctive Imaging Tool in the Evaluation of Treatment Response of Brain Metastases Following Stereotactic Radiosurgery, Medical Research Archives, [online] 10(6). https://doi.org/10.18103/mra.v10i6.2807

Copyright: © 2022 European Society of Medicine. This is an open- access article distributed under the terms of the Creative Commons Attribution License, which permits unrestricted use, distribution, and reproduction in any medium, provided the original author and source are credited.

DOI
https://doi.org/10.18103/mra.v10i6.2807

ISSN: 2375-1924

RESEARCH ARTICLE

High-Resolution Intratumoral Susceptibility Signal (ITSS) as an Adjunctive Imaging Tool in the Evaluation of Treatment Response of Brain Metastases Following Stereotactic Radiosurgery

Ayman Nada, MD, PhD[1]; Esmat Mahmoud, MD, PhD[2]; Humera Ahsan, MD[3]; Gregory Biedermann, MD[1]; Joseph P. Cousins, MD, PhD[3]*

[1] Assistant Professor of Clinical Radiology, Department of Radiology, University of School of Medicine, Columbia, Missouri. 65212
[2] Attending, Diagnostic and Interventional Radiology Department, National Cancer Institute, Cairo University, Egypt
[3] Professor of Clinical Radiology, Department of Radiology, University of School of Medicine, Columbia, Missouri. 65212

* cousinsj@health.missouri.edu

ABSTRACT

Purpose: To evaluate the longitudinal change of intra-tumoral susceptibility signal (ITSS) on high-resolution SWI as an adjunctive imaging tool to evaluate treatment response of brain metastasis following stereotactic radiosurgery. This approach will allow further stratification of the patients and guide clinical decision making.

Methods: An IRB approved retrospective study included 63 brain metastatic lesions within 49 patients (33 females and 16 males) who have undergone stereotactic radiosurgery with at least one follow-up MRI and available clinical data. The average age was 63.17 years (±1.48, ranged from 34-83 years). The longitudinal change in ITSS was categorized into 3 groups; increased, stable and decreased. The treatment response of each lesion was evaluated according to the longitudinal change in size, enhancement and susceptibility at the baseline and follow-up MRIs. Chi-square test was used to compare differences in categorical variables. Receiver operating characteristics (ROC) curve was used to evaluate the accuracy of including longitudinal change in ITSS with size and enhancement pattern in determining the treatment response following SRS.

Results: Our results demonstrated higher sensitivity and specificity when including longitudinal change in ITSS with size and enhancement for the evaluation of the treatment response of brain metastatic lesions treated with SRS. There was statistically significant difference between the different ITSS and enhancement patterns at baseline and follow-up MRIs (Wilcoxon Signed Ranks Test ($p = .000$, and $.003$) respectively. The multiparametric analysis of the longitudinal change in size, contrast enhancement, and ITSS in the evaluation of treatment response in the follow-up MRIs, showed that the sensitivity and specificity significantly improved (AUC 0.953).

Conclusion: High resolution SWI can contribute as an imaging biomarker with supplemental information for monitoring treatment and predicting treatment response. High resolution SWI can complement the standard contrast enhanced T1 images to evaluate treatment response with a multiparametric MRI approach.

Introduction:

Brain metastases are the most common intracranial masses in adults with an incidence of up to 65% during the course of illness.[1,2] The incidence of cerebral metastasis ranges from 5-20% and typically depends upon the histological subtype and stage of primary extracerebral tumor.[3–5] Intracranial metastasis is a significant cause of morbidity and mortality in patients with metastatic cancer.[1,2] The most common primary sites are lung, melanoma, renal cell, breast and colorectal cancer.[1,3,4] Lung cancer is the most common intracranial metastasis, and non-small cell lung cancer presents with brain metastases in up to 10% of patients, while as many as 40% will develop brain metastases during the course of their illness.[6] The treatment options of brain metastases are variable, and primarily depends on number of metastatic lesions. Multiple brain metastases typically are treated with hippocampal sparing whole brain radiotherapy which has comorbidities and potential neurocognitive decline.[7–10] Oligo-metastases can be treated with surgical resection, stereotactic radiosurgery or combination of both.[3] Stereotactic radiosurgery (SRS) is the mainstay for treatment of oligometastases in patients with good performance status.[11–13]

Due to the high inherent soft tissue contrast, Magnetic Resonance Imaging (MRI) is the imaging modality of choice for evaluation of primary and metastatic brain tumors, post-surgical and therapeutic surveillance, and for monitoring treatment response.[14,15] The conventional MRI sequences such as T2 FLAIR and post contrast T1 lack specificity to differentiate between local progression versus radiation changes, and also lack predictive value.[16,17] Therefore, there is a need to investigate other imaging parameters that may improve the sensitivity and specificity of response to treatment at baseline, and/or follow up, and potentially reduce the exposure to contrast agents.

Susceptibility-weighted imaging (SWI) is an MRI sequence that utilizes the magnetic susceptibility differences between tissues.[18] Spoiled gradient-echo sequences use both magnitude and phase images, which provide high sensitivity for the detection of blood degradation products, calcifications, and iron deposits.[19] High-resolution SWI provides visualization of small vessels, can detect iron deposition, and can generate image contrast depending on magnetic susceptibility differences in tissues.[18] The phase images further help to differentiate between paramagnetic materials like iron which have strong positive susceptibility phase, from diamagnetic materials like calcium which have negative susceptibility phase.[20] (For those not familiar with MRI physics, positive phase is similar to the crest of a wave; negative phase the trough.) High-resolution SWI sequences are increasingly utilized to help narrow differential diagnosis in neuroimaging.[18] SWI has proven to be excellent in evaluation of traumatic brain injury with detection of discrete punctate microhemorrhage and diffuse axonal injury.[21–23] SWI has become an imperative imaging technique for evaluation of ischemic cerebral stroke with differentiation of hemorrhagic and non-hemorrhagic acute strokes.[24–26] Based on these findings, SWI has been integrated into standard routine MRI protocols for evaluation of the brain. Furthermore, many research groups have investigated thoroughly the utility of SWI and reconstructed quantitative susceptibility mapping (QSM) in the evaluation of neurodegenerative disorders with special focus on Alzheimer.[27–31]

High-resolution SWI and transverse relaxation rate, R2*, mapping have been found to be promising for differentiation of tumor progression from pseudo-progression in patients with glioblastoma. R2* was higher in the contrast and non-contrast regions for the tumor progression group than pseudo-progression group.[32] R2* was reported to have high sensitivity for detection of radiation-induced changes in animal models, with promising role in differentiating tumor progression from radiation necrosis.[33,34] Percentage wise quantification of ITSS has been investigated to differentiate between brain metastases. It was successful for differentiation between brain metastases of malignant melanoma form those of breast and lung cancers.[35]

SRS causes endothelial cell death with vascular consequences, i.e. increased permeability, decreased blood flow, and hypoxia.[36] Increased susceptibility can be observed in non-specific micro-bleedings, or post treatment tumoral remnants.[37] These changes could be evaluated on SWI following SRS which allow for the assessment of treatment response along with T1 post-contrast images.[38,39] The purpose of our study was to extend previous work and evaluate the longitudinal change of intratumoral susceptibility signal (ITSS) on high-resolution SWI as an adjunctive imaging tool to evaluate treatment response of brain metastasis following stereotactic radiosurgery. Our hypothesis is that this approach could help further stratification of the patients and guide clinical decision making.

Methods:

Study population:

This IRB approved, retrospective study included 49 patients from our institute (with 63 metastatic brain lesions) who presented at our medical center to the radiation oncology, neurosurgery, or hematology-oncology clinics with brain metastases. A search on our PACS system for MRIs with indication "brain metastasis" yielded 502 MRI scans from November 2016 to August, 2020. After exclusion of repeated patients, patients with other diagnosis (e.g. glioblastoma, meningioma, etc.), and patients without complete clinical data, the final study cohort included 49 patients (33 women and 16 men) with 63 brain metastatic lesions. The patients had undergone stereotactic radiosurgery with at least one follow-up MRI and had appropriate clinical data. The average age was 63.2 ±1.5 yrs (age range 34-83 yrs). The average age of men was 67 years; the average age of women was 60.8 years.

The patients underwent treatment with SRS, either as the main treatment armamentarium, or following post-surgical resection of one or more dominant metastatic brain lesions.

- *Inclusion criteria:*
  - Patients with brain metastases who received stereotactic radiosurgery as a definitive treatment.
  - Patients who underwent surgical resection of the dominant brain metastases with completion SRS for the remaining lesions.
- *Exclusion criteria:*
  - Patients who underwent definitive surgical treatment for a solitary resectable brain metastasis.
  - Pediatric population (patients < 18 years).

Imaging techniques and MRI protocol:

All patients had base-line diagnostic MRI including high-resolution susceptibility weighted images, along with pre and post intravenous gadolinium-based contrast administration 3D T1 magnetization-prepared 180 degrees radio-frequency pulses and rapid gradient-echo (MPRAGE). MRI exams were performed on our 3 Tesla MR scanners (MAGNETOM Vida and Skyra, Siemens Healthineers, USA) using 30 and 20 channel head coils respectively. The MRI protocol is summarized in Table. 1.

Automated post processing of the SWI acquisition provided the phase, MIP, and magnitude images. The phase images help to differentiate paramagnetic iron from diamagnetic calcium materials.

Imaging evaluation:

The primary tumor pathology, the date of initial diagnosis, and the development of brain metastasis were tracked. Brain metastases were evaluated according to location, size, and signal characteristics in different MRI sequences. The maximal axial perpendicular diameters and volume of each lesion were obtained.

Qualitative evaluation of each brain metastatic lesion on SWI: The imaging pattern of ITSS, the morphology, and signal intensity were obtained within each brain metastasis. Paramagnetic materials as iron were differentiated from diamagnetic materials such as calcium using SWI phase images. The imaging patterns of ITSS were categorized by two board certified, diplomat neuroradiologists (JPC, and HA, with 15 and 20-year experience respectively) independently, with each brain metastasis lesion categorized into 3 groups: *increased, decreased or stable,* according to the visual evaluation of the longitudinal change in intra-tumoral susceptibility between the baseline and follow-up MRIs (Figs. 1, and 2).

Table. 1: MRI parameters of different sequences including SWI and 3D T1 MPRAGE with IV contrast administration.

Sequence	TE (ms)	TR (ms)	TI (ms)	Flip Angle	Slice Thickness	Matrix
Axial T2	97	5		150 °	5 mm	256 x 256 x 16
Axial FLAIR	90	7	2220	150 °	5 mm	512 x 512 x 16
Sag 3D T1 MPRAGE	3	2300	900	150 °	1 mm	256 x 248 x 16
Axial DWI	83	4400		90 °	5 mm	260 x 260 x 16
Axial SWI	20	27		15°	3mm	256 x 256 x 16
Sag T1 MPRAGE + C	2.5	2300		8 °	1 mm	256 x 256 x 16

Figure. 1: Axial SWIs and 3D T1 MPRAGE with IV contrast at baseline (A, and C) and follow-up (B, and D) demonstrate good therapeutic response after SRS (arrows).

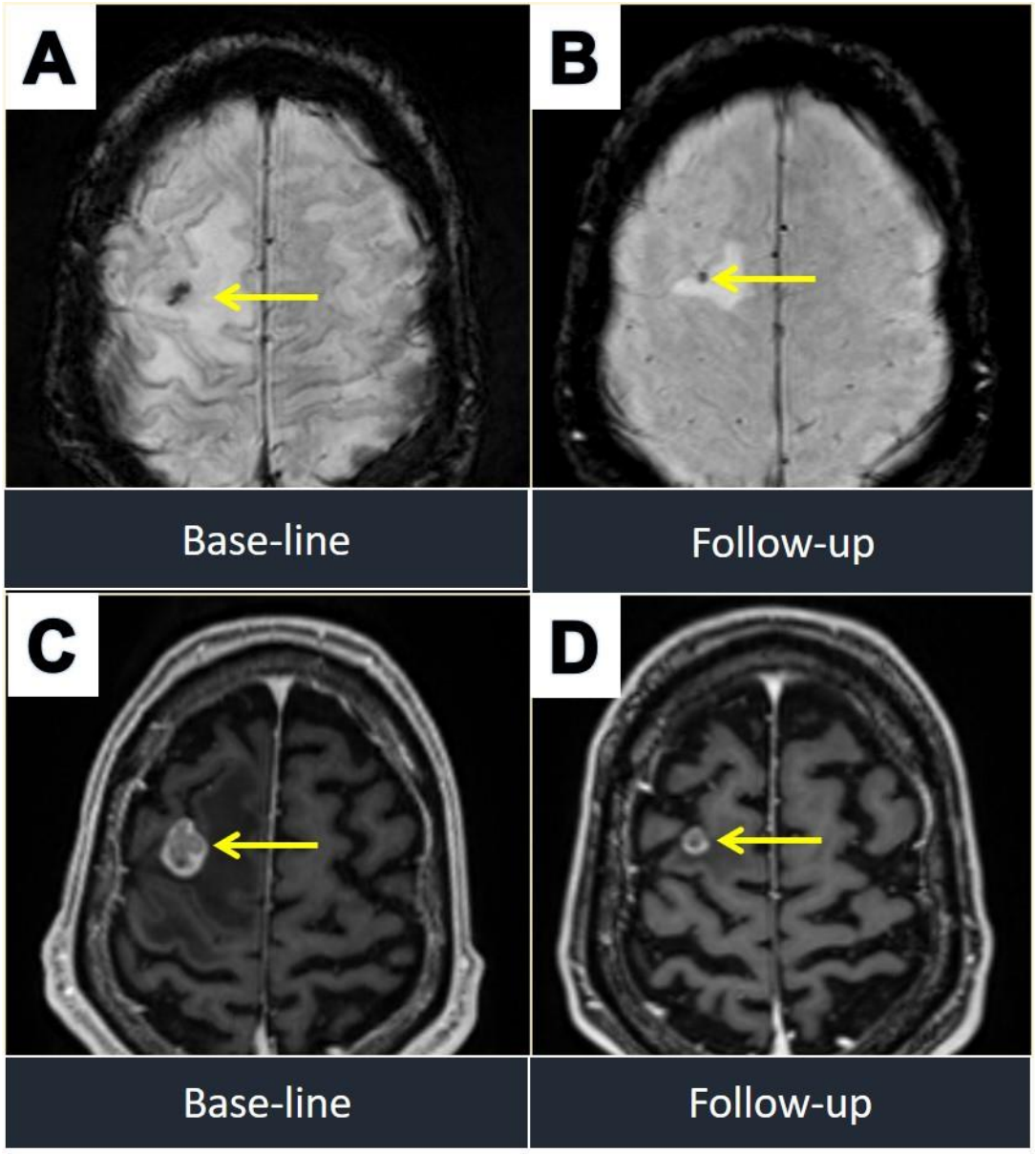

Figure. 2: Axial SWIs and 3D T1 MPRAGE with IV contrast at baseline (A, and C) and follow-up (B, and D) demonstrate an example of pseudoprogression after SRS (arrows).

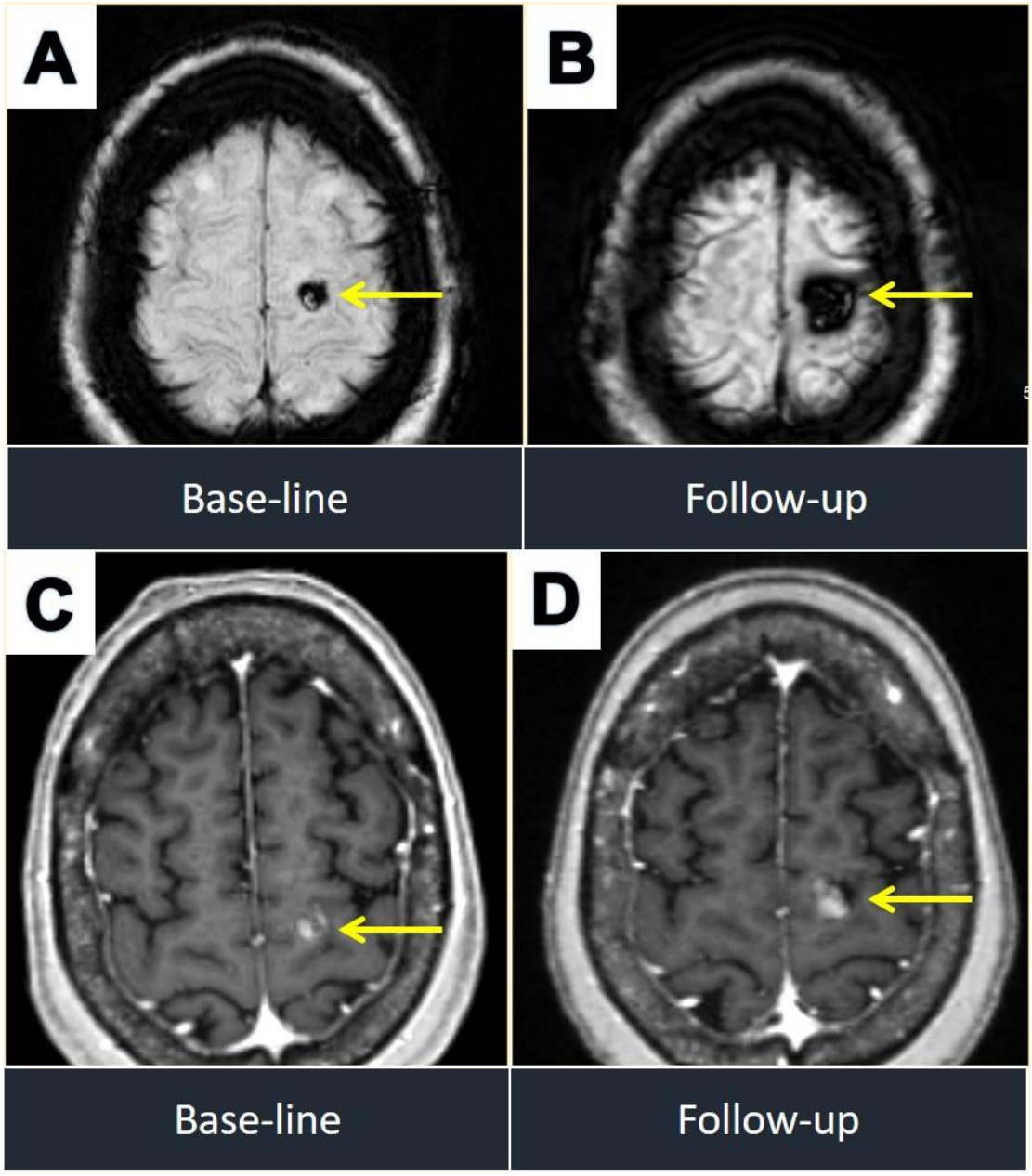

Evaluation of the enhancement pattern of each lesion: The degree of enhancement of each brain metastasis was also evaluated and categorized into 3 groups by the neuroradiologists: *increased, decreased or stable* according to the longitudinal change between the baseline and follow-up MRIs.

Correlation with treatment response: Treatment response of each lesion was correlated with the clinical status of the patient obtained from the electronic medical records (EMR). The patients were then classified into 2 groups: 1) positive or good treatment response; 2) negative or non-favorable treatment response. The positive treatment response group was determined based on clinical improvement of the symptoms, reduction or withdrawal of the corticosteroid therapy, or follow-up/observation of without further intervention. The non-favorable treatment response group was selected when the patient's symptoms worsened, increase in corticosteroid dose was needed, or another treatment modality, e.g. surgical resection, was employed. Receiver Operating Curve (ROC)

analysis was performed to predict the treatment response based on the longitudinal change in the degree of enhancement, and then combined with the longitudinal change in ITSS. This approach evaluated the additive role and substantial value of SWI when combined with the degree of change in enhancement.

Stereotactic Radiosurgery Protocol:

All patients underwent stereotactic radiation therapy with either single fraction radiosurgery, or multi-fraction stereotactic treatments. For SRS treatments, all patients had a CT for simulation calculations and targeting. An open-faced thermoplastic mask (Qfix, Avondale, PA) for immobilization was employed. The 3D T1 MPRAGE MRI post contrast images were fused to the CT images using a rigid fusion algorithm. The gross target volumes (GTV) were then contoured by a neurosurgeon, calculated by a radiation oncologist physicist, and reviewed by the radiation oncologist. Depending on the size of the metastases and the locations, either 1, 3 or 5 fractions were prescribed. Treatment planning was performed on Eclipse Treatment Planning System (Varian, Palo Alto, CA) and doses were prescribed to the planning target volume (PTV) with a 2mm margin around the GTV. Typical doses were 15 Gy for single fraction, 24 Gy in 3 fractions, or 30 Gy in 5 fractions. For a single lesion, 3D conformal, multi-field non-coplanar beams were used. For multiple metastases, volume modulated arc therapy (VMAT) was used, with 4 or 5 non-coplanar arcs. The treatments were performed on the Varian Trilogy with pre-treatment cone beam CT used for image guidance. Patient positioning was adjusted using a 6-degrees of freedom tabletop, and position was verified during the treatment using the VisionRT (VisionRT, London, UK) system.

Statistical analysis:

Statistical analysis was performed using Microsoft Excel and IBM SPSS 26 software. The mean and standard deviation were used for numeric data e.g., age, maximal axial perpendicular diameters of the brain metastatic lesions, and ADC values. The data was tested for normality by the Kolmogrov-Samironov test. Paired t-test and one sample t-test were used for normally distributed data; Mann Whitney and Wilcoxon signed rank tests were used for non-normally distributed data. Chi square and Fisher exact tests were used for categorical variables. The accuracy, specificity, and sensitivity with ROC curve and AUC was calculated.

Results:

Longitudinal changes of ITSS on high-resolution SWI: Statistically significant changes in the imaging patterns of ITSS on high-resolution SWI were found between the baseline and follow up MRI exams using Wilcoxon Signed Ranks Test ($p < .001$). The different imaging patterns of ITSS on the post SRS MRI exams were compared to treatment responses which also had statistical significance, $p = 0.037$ (Mann Whitney U test, Exact significance (1-tailed). The changes in ITSS had a high sensitivity and positive predictive value of 90.91% for each category, with lower specificity 78.95%. The overall accuracy was 87.3%

We did not find any statistically significant difference among the groups according to gender or age. We obsereved slight increase in the accumulation of susceptibility signal with time in women, however, there was no statistical significance in longitudinal change of ITSS on high-resolution SWI on follow up MRIs between women and men ($\chi^2 = 0.446$, p-value = 0.8), or different age groups (p-value = 0.963).

Longitudinal changes in Gadolinium enhancement patterns on CE-3D T1 MPRAGE:

Qualitative evaluation of post contrast 3D T1 MPRAGE series was performed, classified into 3 groups, based on longitudinal changes in enhancement: Increased, Stable, and Decreased. The longitudinal change of enhancement pattern of brain metastases between baseline and follow up MRIs was statistically significant ($p = .003$, Wilcoxon Signed Ranks Test, Exact Sig., 2-tailed, Fig.3A). There was also a statistically significant difference between the groups according to treatment response ($p = 0.007$, Fig 3B). There was no statistical significance in the longitudinal change of enhancement pattern of the tumors on follow up MRIs between women and men ($\chi^2 = 5.064$, p-value = 0.079), or different age groups (p-value = 0. 374).

Figure. 3: ROC curve for comparison of the treatment response regarding the longitudinal change in size, enhancement and ITSS

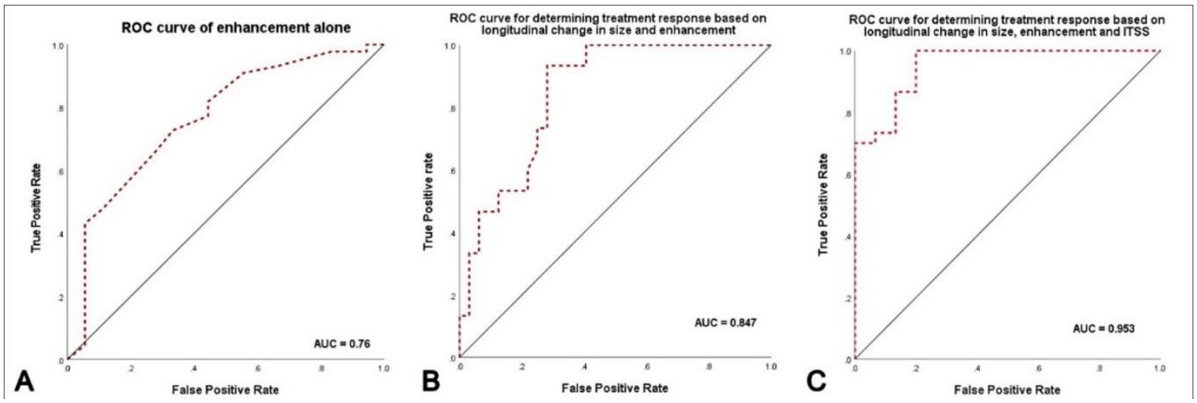

Combined evaluation of brain metastases regarding longitudinal change in size, enhancement and ITSS patterns:

The multiparametric analysis of the longitudinal change in size, contrast enhancement, and ITSS in the evaluation of treatment response in the follow-up MRIs, showed that the sensitivity and specificity significantly improved (AUC 0.953, Fig. 3C).

Discussion:

Traditional evaluation of the treatment response of brain metastases relies primarily in the change enhancement pattern and size and of brain tumors.[40,41] Confounding factors affect the enhancement pattern and size of the treated tumors, i.e. the use of steroids, SRS fields and dosages, and other new target therapies.[42,43] Therefore, measuring the size of enhancement alone lacks the required sensitivity and specificity to evaluate treatment response.

Multiparametric MRI evaluations have the potential to increase sensitivity and specificity for determining treatment response and help appropriate management.[41,44–46] One of the promising sequences is susceptibility weighted imaging.[37] High-resolution SWI is sensitive to microvasculature changes due to the composition of oxy/deoxyhemoglobin, blood products from microhemorrhages, and iron accumulation due to recruitment of iron-laden macrophages.[37,47] SWI has gained popularity for the evaluation of a wide spectrum of neurologic disorders. We have investigated its value as an adjunctive tool in the evaluation of brain metastasis following SRS. SWI has gained popularity for the evaluation of a wide spectrum of neurologic disorders. We have investigated its value as an adjunctive tool in the evaluation of brain metastasis following SRS.

Our results demonstrate the potential value in combining the changes in ITSS with the degree of enhancement in predicting and determining the treatment response of brain metastases following SRS.

SWI has been investigated to predict brain tumors, differentiate primary brain tumors and brain metastasis, and differentiate brain metastases.[19,37,39,48] Radbruch, et al. have investigated quantitative measurement of SWI using percentagewise quantification for the discrimination of intracerebral metastases. They found excellent diagnostic performance of the PQ of ITSS to differentiate malignant melanoma and breast carcinoma (AUC= 0.96; 95% CI 0.9 – 1.0).[35] Those results were promising and our goal was to extend that research and investigate the utility of SWI to evaluate treatment response and predict patients' prognosis for the treatment of metastases regardless of type. Our study supports the findings of Radbruch, et al. [35], and strongly indicates that the qualitative assessment of ITTS and the changes following SRS follow morphological imaging patterns which correspond to treatment response, and potentially could affect clinical decision making (Fig. 3C, 4). Pinker et al. demonstrated a correlation between intratumoural susceptibility effects, positron emission tomography (PET) results and histopathological grading.[49] Due to its ability to detect the intratumoral microvasculature, SWI has been proposed as a helpful tool in the evaluation of clinical outcome to anti-angiogenetic treatment with better prediction of pseudo-progression phenomenon after concurrent chemo- and radiotherapy.[50,51]

Figure. 4: Flow chart illustrating the design strategy and how our approach can guide clinical decision making

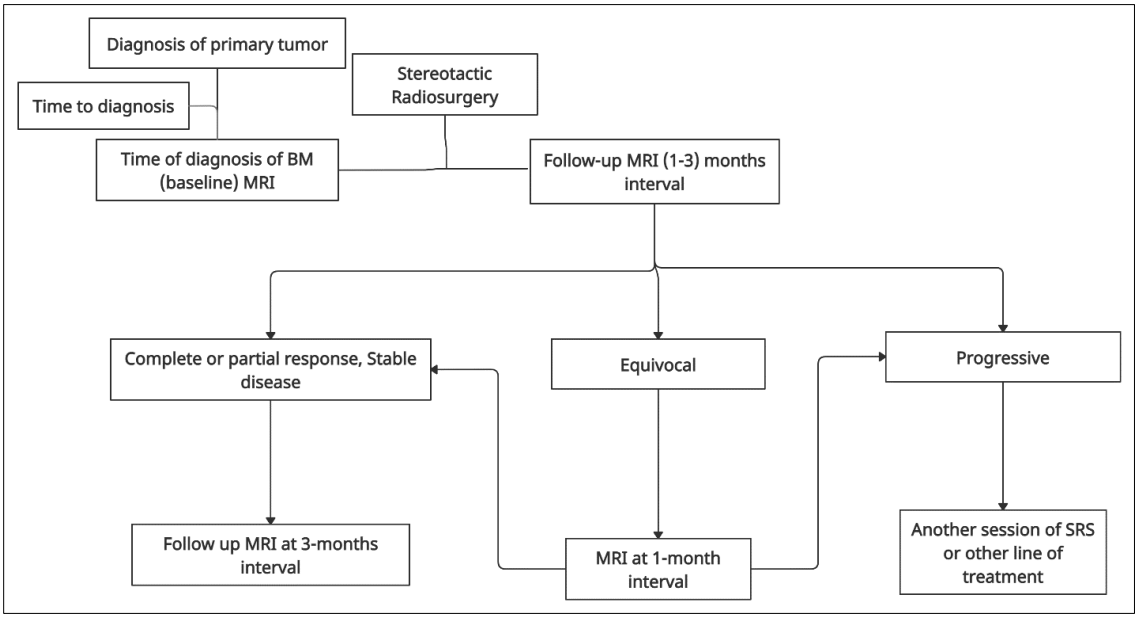

SWI also has been helpful for delineation of the inner boundaries of tumors which allow for better surgical planning and improved clinical outcomes.[52] Interestingly Kong et al have found significant correlation between ITSS grade and prediction of glioma grade, IDH mutation and MGMT promoter methylation status.[53] Brain metastasis encompass a wide range of heterogenous disease but studying the association of ITSS grade to underlying genetic mutations such as EGFR would impact management plan and patient care. Neverthless one sequence or imaging technique can stand-alone and provide optimal and accurate evaluation of treatment outcome in the patients with brain metastases after SRS. Multi-parametric approach with including information of each sequence would be helpful for better evaluation and explanation of the biochemical derangement within the tumor microenvironment after therapy. Therefore, we proposed that careful evaluation of the intratumoral susceptibility signal (ITSS) could act as an adjunctive imaging tool for the evaluation of treatment outcomes following SRS. Evaluation of ITSS can be qualitative or quantitative. Quantitative methods with voxel-based morphometry techniques and accurate measurement of ITSS would further improve the evaluation of treatment outcomes and allow for a standard replicable tool for daily practice.

CE-MRI is the standard of care for the evaluation of treatment response of brain metastases.[41,44,46] The SRS treatment-induced changes on the tumor microenvironment usually occur early following therapy. These microstructural changes are not routinely depicted before there is a radiographic perceptible change in tumor size or volume by conventional MRI. Advanced MRI sequences such as SWI and diffusion weighted images can provide additional information about the microstructural changes, which in our study, strongly correlated with response to therapy. Magnetic resonance perfusion and spectroscopy potentially could provide additional biochemical information and changes within metastases which may contribute to prediction of tumor response before traditional radiographic morphological changes.

Limitations of the study:

One limitation of this study is the sample size. A larger study with a larger population is needed to validate these results. Because of the sample size, we could not obtain statistical power for potential subsets of imaging patterns of ITSS, which could potentially correlate with different degrees of treatment response and tumor categories. Further research would emphasize the differences in imaging patterns of ITSS for treated brain metastatic lesions. Additionally, the classifications of these imaging patterns would need confirmation at other sites before gaining wide acceptance in the neuroradiology community.

Conclusion:

High resolution SWI can contribute as an imaging biomarker with supplemental information for monitoring treatment and predicting treatment response. Our results corroborate those of other researchers. High resolution SWI can complement the standard contrast enhanced T1 images to evaluate treatment response with a multiparametric MRI approach. We have demonstrated that the combination of high resolution SWI and CE-MRI improves the neuroradiologist's ability to distinguish positive treatment response from tumor progression, and can potentially have a positive effect on clinical management.

References:

1. Soliman, H., Das, S., Larson, D. A. & Sahgal, A. Stereotactic radiosurgery (SRS) in the modern management of patients with brain metastases. *Oncotarget* 7, 12318–12330 (2016).
2. Taunk, N. K. *et al*. Early posttreatment assessment of MRI perfusion biomarkers can predict long-term response of lung cancer brain metastases to stereotactic radiosurgery. *Neuro-Oncology* 20, 567–575 (2018).
3. Lohmann, P. *et al*. PET/MRI Radiomics in Patients With Brain Metastases. *Frontiers in Neurology* vol. 11 1 (2020).
4. Nayak, L., Lee, E. Q. & Wen, P. Y. Epidemiology of brain metastases. *Current Oncology Reports* 14, 48–54 (2012).
5. Kniep, H. C. *et al*. Radiomics of brain MRI: Utility in prediction of metastatic tumor type. *Radiology* 290, 479–487 (2019).
6. Lin, C. Y. *et al*. Brain MRI imaging characteristics predict treatment response and outcome in patients with de novo brain metastasis of EGFR-mutated NSCLC. *Medicine (United States)* 98, (2019).
7. Singh, C., Qian, J. M., Yu, J. B. & Chiang, V. L. Local tumor response and survival outcomes after combined stereotactic radiosurgery and immunotherapy in non-small cell lung cancer with brain metastases. *Journal of Neurosurgery* 132, 512–517 (2020).
8. Aoyama, H. *et al*. Stereotactic radiosurgery plus whole-brain radiation therapy vs stereotactic radiosurgery alone for treatment of brain metastases: A randomized controlled trial. *J Am Med Assoc* (2006) doi:10.1001/jama.295.21.2483.
9. Chang, E. L. *et al*. Neurocognition in patients with brain metastases treated with radiosurgery or radiosurgery plus whole-brain irradiation: a randomised controlled trial. *The Lancet Oncology* (2009) doi:10.1016/S1470-2045(09)70263-3.
10. Lohmann, P. *et al*. Combined FET PET/MRI radiomics differentiates radiation injury from recurrent brain metastasis. *NeuroImage: Clinical* 20, 537–542 (2018).
11. Suh, J. H. *et al*. Current approaches to the management of brain metastases. *Nature Reviews Clinical Oncology* 17, 279–299 (2020).
12. Ong, W. L., Wada, M., Ruben, J., Foroudi, F. & Millar, J. Contemporary practice patterns of stereotactic radiosurgery for brain metastasis: A review of published Australian literature. *Journal of Medical Imaging and Radiation Oncology* 63, 711–720 (2019).
13. Rosenfelder, N. & Brada, M. Integrated treatment of brain metastases. *Current Opinion in Oncology* 31, 501–507 (2019).
14. Langen, K. J. & Galldiks, N. Update on amino acid pet of brain tumours. *Current Opinion in Neurology* (2018) doi:10.1097/WCO.0000000000000574.
15. Langen, K. J., Galldiks, N., Hattingen, E. & Shah, N. J. Advances in neuro-oncology imaging. *Nature Reviews Neurology* (2017) doi:10.1038/nrneurol.2017.44.
16. Lin, N. U. *et al*. Response assessment criteria for brain metastases: Proposal from the RANO group. *The Lancet Oncology* (2015) doi:10.1016/S1470-2045(15)70057-4.
17. Okada, H. *et al*. Immunotherapy response assessment in neuro-oncology: A report of the RANO working group. *The Lancet Oncology* (2015) doi:10.1016/S1470-2045(15)00088-1.
18. Halefoglu, A. M. & Yousem, D. M. Susceptibility weighted imaging: Clinical applications and future directions. *World J Radiol* 10, 30–45 (2018).
19. Roh, K., Kang, H. & Kim, I. Clinical Applications of Neuroimaging with Susceptibility Weighted Imaging: Review Article. *Journal of the Korean Society of Magnetic Resonance in Medicine* 18, 290 (2014).
20. Ruetten, P. P. R., Gillard, J. H. & Graves, M. J. *introduction to Quantitative Susceptibility Mapping and Susceptibility weighted imaging*. (2019).
21. Tate, D. F. *et al*. Susceptibility Weighted Imaging and White Matter Abnormality Findings in Service Members With Persistent Cognitive Symptoms Following Mild Traumatic Brain Injury. *MILITARY MEDICINE* 182, e1651–e1658 (2017).
22. Huang, Y.-L. *et al*. *Susceptibility-weighted MRI in mild traumatic brain injury From the*

Department of Diagnostic Radiology (Y. (2015).

23. Bigler, E. D., Maxwell, W. L., Bigler, E. D. & Maxwell, W. L. Neuropathology of mild traumatic brain injury: relationship to neuroimaging findings. *Brian Imaging and Behavior* 6, 108–136 (2012).
24. Darwish, E. A. F., Abdelhameed-El-Nouby, M. & Geneidy, E. Mapping the ischemic penumbra and predicting stroke progression in acute ischemic stroke: the overlooked role of susceptibility weighted imaging. *Insights into Imaging* 11, 1–8 (2020).
25. Luo, S., Yang, L. & Luo, Y. Susceptibility-weighted imaging predicts infarct size and early-stage clinical prognosis in acute ischemic stroke. *Neurological Sciences* 39, 1049–1055 (2018).
26. Hsu, C. C.-T. *et al*. Susceptibility weighted imaging in acute cerebral ischemia: review of emerging technical concepts and clinical applications. *Neuroradiol J* 30, 109–119 (2017).
27. 790 Kim et al. Susceptibility changes in SAD Quantitative Magnetic Susceptibility Assessed by 7T Magnetic Resonance Imaging in Alzheimer's Disease Caused by Streptozotocin Administration. *Quantitative Imaging in Medicine and Surgery* 10, 789–797 (2020).
28. O'callaghan, J. *et al*. Tissue magnetic susceptibility mapping as a marker of tau pathology in Alzheimer's disease. *Neuroimage* 159, 334–345 (2017).
29. Acosta-Cabronero, J. *et al*. In Vivo Quantitative Susceptibility Mapping (QSM) in Alzheimer's Disease. *PLoS ONE* 8, e81093–e81108 (2013).
30. Kim, H.-G. *et al*. Quantitative susceptibility mapping to evaluate the early stage of Alzheimer's disease ☆. *NeuroImage: Clinical* 16, 429–438 (2017).
31. Li, D. T. H. *et al*. Quantitative susceptibility mapping as an indicator of subcortical and limbic iron abnormality in Parkinson's disease with dementia. *NeuroImage: Clinical* 20, 365–373 (2018).
32. Belliveau, J. G. *et al*. Apparent transverse relaxation (R2∗) on MRI as a method to differentiate treatment effect (pseudoprogression) versus progressive disease in chemoradiation for malignant glioma. *Journal of Medical Imaging and Radiation Oncology* 62, 224–231 (2018).
33. Prediction of radiation necrosis in a rodent model using magnetic resonance imaging apparent transverse relaxation ( ). *Physics in Medicine & Biology* 63, 035010 (9pp) (2018).
34. Jenrow, K. A. *et al*. Selective Inhibition of Microglia-Mediated Neuroinflammation Mitigates Radiation-Induced Cognitive Impairment. (2013) doi:10.1667/RR3026.1.
35. Radbruch, A. *et al*. Differentiation of brain metastases by percentagewise quantification of intratumoral-susceptibility-signals at 3 Tesla. *European Journal of Radiology* 81, 4064–4068 (2012).
36. Nivet, A., Schlienger, M., Clavère, P. & Huguet, F. Effects of high-dose irradiation on vascularization: Physiopathology and clinical consequences. *Cancer radiotherapie : journal de la Societe francaise de radiotherapie oncologique* 23, 161–167 (2019).
37. Adi Vachha, B. *et al*. Clinical Value of Susceptibility Weighted Imaging of Brain Metastases. *Frontiers in Neurology | www.frontiersin.org* 11, 55 (2020).
38. Kang, H. & Jang, S. The diagnostic value of postcontrast susceptibility-weighted imaging in the assessment of intracranial brain neoplasm at 3T. *Acta Radiologica* (2020) doi:10.1177/0284185120940265.
39. Schwarz, D. *et al*. Susceptibility-weighted imaging in malignant melanoma brain metastasis. *Journal of Magnetic Resonance Imaging* 50, 1251–1259 (2019).
40. Silbergeld, D., Fink, K. R. & Fink, J. R. Surgical Neurology International Surgical Neurology International SNI: Neuro-Oncology, a supplement to Surgical Neurology International OPEN ACCESS Imaging of brain metastases. doi:10.4103/2152-7806.111298.
41. Huang, S. Y. *et al*. Advanced Imaging of Brain Metastases: From Augmenting Visualization and Improving Diagnosis to Evaluating Treatment Response. *Frontiers in Neurology | www.frontiersin.org* 1, 270–284 (2020).

42. Niranjan, A., Dade Lunsford, L. & Ahluwalia, M. S. Targeted therapies for brain metastases. *Progress in Neurological Surgery* **34**, 125–137 (2019).
43. Masoud, V. & Pagès, G. Targeted therapies in breast cancer: New challenges to fight against resistance World Journal of Clinical Oncology. *World J Clin Oncol* **8**, 120–134 (2017).
44. Pope, W. B. Brain metastases: neuroimaging. *Handb Clin Neurol* **149**, 89–112 (2018).
45. Liu, Q., Tong, X. & Wang, J. Management of brain metastases: history and the present. *Chinese Neurosurgical Journal* **5**, 1–8 (2019).
46. di Ieva, A. *et al*. Advanced Magnetic Resonance Imaging Techniques in Management of Brain Metastases. *Front. Oncol* **9**, 440–456 (2019).
47. Lee, J., Hirano, Y., Fukunaga, M., Silva, A. C. & Duyn, J. H. On the contribution of deoxy-hemoglobin to MRI gray-white matter phase contrast at high field. *Neuroimage* **49**, 193–198 (2010).
48. Sawlani, V. *et al*. Evaluation of Response to Stereotactic Radiosurgery in Brain Metastases Using Multiparametric Magnetic Resonance Imaging and a Review of the Literature. *Clinical Oncology* **31**, 41–49 (2019).
49. Pinker, K. *et al*. High-Resolution Contrast-Enhanced, Susceptibility-Weighted MR Imaging at 3T in Patients with Brain Tumors: Correlation with Positron-Emission Tomography and Histopathologic Findings. doi:10.3174/ajnr.A0540.
50. Al, A. *et al*. Distinguishing Recurrent Primary Brain Tumor from Radiation Injury: A Preliminary Study Using a Susceptibility-Weighted MR ImagingGuided Apparent Diffusion Coefficient Analysis Strategy. doi:10.3174/ajnr.A2011.
51. Gasparotti, R., Pinelli, L. & Liserre, R. New MR sequences in daily practice: susceptibility weighted imaging. A pictorial essay. *Insights into Imaging* **2**, 335 (2011).
52. Mittal, S., Wu, Z., Neelavalli, J. & Haacke, E. M. Susceptibility-weighted imaging: Technical aspects and clinical applications, part 2. *American Journal of Neuroradiology* vol. 30 232–252 (2009).
53. Kong, L.-W. *et al*. intratumoral Susceptibility Signals Reflect Biomarker Status in Gliomas. *Scientific RepoRtS* | **9**, 17080 (2019).